International Journal of Food Microbiology 432 (2025) 111096

Contents lists available at ScienceDirect

International Journal of Food Microbiology

journal homepage: www.elsevier.com/locate/ijfoodmicro

Characterising phages for the control of pathogenic bacteria associated with bivalve consumption

Pedro Costa [a], Carla Pereira [a], Vanessa Oliveira [a], Newton C.M. Gomes [a], Jesús L. Romalde [b], Adelaide Almeida [a,*]

[a] CESAM, Department of Biology, University of Aveiro, Campus Universitário de Santiago, 3810-193 Aveiro, Portugal
[b] Department of Microbiology and Parasitology, CRETUS & CIBUS - Faculty of Biology, University of Santiago de Compostela, CP 15782 Santiago de Compostela, Spain

ARTICLE INFO

Keywords:
Bacteriophages
Pathogenic bacteria
Bivalve consumption
Phage biocontrol

ABSTRACT

In the present study, five new bacteriophages (or phages) were characterized, and their efficacy in controlling pathogenic bacteria—*Escherichia coli*, *Salmonella enterica* serovar Typhimurium, *Salmonella enterica* serovar Enteritidis, *Aeromonas hydrophila*, and *Vibrio parahaemolyticus*—associated with bivalve consumption was evaluated. The isolated phages include both siphovirus [vB_EcoS_UALMA_PCEc3 (PCEc3), vB_SeTS_UALMA_PCST1 (PCST1), and vB_VpaS_UALMA_PCVp3 (PCVp3)] and myovirus [vB_SeEM_UALMA_PCSE1 (PCSE1) and vB_AhyM_UALMA_PCAh2 (PCAh2)] morphotypes. Four phages are safe for bacterial control, with only one (PCAh2) showing potential lysogenic characteristics. All phages exhibited a narrow host range, capable of infecting up to six additional bacterial strains besides their original host, and four could infect the host bacteria of other phages. Adsorption rates ranged from 24% and 98% within 1 h. One-step growth assays revealed different latent periods, ranging from 10 to 120 min, and low to average burst sizes, ranging from 7.60 to 83.97 PFU/mL. Generally, increasing the multiplicity of infection (MOI) enhanced phage efficiency significantly. All phages effectively reduced the bacterial load of their respective hosts, achieving maximum reductions between 3.73 and 5.57 log CFU/mL within 10 h of treatment. These results suggest that phage biocontrol can be an effective alternative to combat pathogenic bacteria associated with bivalve consumption.

1. Introduction

Bivalves play a vital role in the human diet, and their commercial value is steadily increasing worldwide (FAO, 2024). In 2022, global exports of bivalve molluscs reached USD 6.0 billion, accounting for approximately 3% of total global aquatic animal product exports and 11% of the overall production from world fisheries and aquaculture (FAO, 2024). Aquaculture production surpassed capture fisheries for the first time in 2022, increasing by 6.7 million tonnes (7.6%) from 2020, with molluscs accounting for 1 million tonnes (15.6%) (FAO, 2024). Global mollusc production in aquaculture steadily increased from 17.5 million tonnes in 2018 to 18.9 million tonnes in 2022 (FAO, 2024). Despite this growth, bivalve prices are rising across major markets due to inflation and high demand, potentially leading to increased consumer resistance amid ongoing economic challenges (FAO, 2024).

Bivalve molluscs filter large volumes of seawater, accumulating particles and potential pathogens which pose significant public health risks (Pereira et al., 2021; Zannella et al., 2017). Seafood-associated pathogenic bacteria can be categorised into three main groups: indigenous marine bacteria like *V. parahaemolyticus* and *A. hydrophila*; enteric bacteria from faecal contamination like pathogenic *E. coli* and *Salmonella* spp.; and bacteria introduced during processing (Iwamoto et al., 2010; Moreno Roldán et al., 2011). These pathogens can cause diseases when shellfish are consumed raw or undercooked (Pereira et al., 2021; Zannella et al., 2017).

Pathogenic *E. coli* strains can contaminate seafood through sewage pollution in coastal environments or post-harvest handling (Kanayama et al., 2015; Potasman et al., 2002). *E. coli* is also used as an indicator for bivalve production zone classification (European Commission, 2004a, 2004b, 2017) and to assess depuration efficiency (Pereira et al., 2017b). *E. coli* infections cause symptoms such as abdominal cramping, watery or bloody diarrhoea, fever, vomiting, and nausea (Kanayama et al., 2015; Potasman et al., 2002).

Salmonella spp., enteric pathogens commonly found in coastal areas,

* Corresponding author.
E-mail address: aalmeida@ua.pt (A. Almeida).

https://doi.org/10.1016/j.ijfoodmicro.2025.111096
Received 22 October 2024; Received in revised form 14 January 2025; Accepted 4 February 2025
Available online 8 February 2025

are a frequent cause of gastroenteritis after consuming contaminated seafood (Kanayama et al., 2015; Potasman et al., 2002). Once introduced into marine environments, *Salmonella* easily contaminates marine life, particularly bivalves, which concentrate marine microorganisms through filter feeding and serve as indicators of depuration efficiency (Lee et al., 2008). *S. enterica* serovar Enteritidis and serovar Typhimurium are among the leading causes of foodborne outbreaks in the United States (Finstad et al., 2012) and the European Union (EFSA and ECDC, 2023). *Salmonella* infections typically cause acute gastroenteritis, with symptoms such as diarrhoea, fever, and abdominal cramps (Pereira et al., 2016a). Other clinical manifestations include bacteremia, enteric fever, urinary tract infections, and severe faecal infections (Pereira et al., 2016a).

Aeromonas hydrophila is widely distributed in aquatic environments and is a typical seafood contaminant (De Silva et al., 2020; De Melo Silva et al., 2014). This bacterium is responsible for a wide range of human infections, including gastroenteritis, pneumonia, wound infections, endocarditis, meningitis, and septicemia, especially in immunocompromised individuals (Butt et al., 2004; Grim et al., 2014).

Vibrio parahaemolyticus is an enteric pathogen commonly found in coastal areas and a leading cause of gastroenteritis in humans following the consumption of contaminated seafood (Potasman et al., 2002). It ranks among the most widespread seafood-associated pathogenic bacteria globally, frequently found in oysters in China (Chen et al., 2010; Drake et al., 2007). Vibriosis outbreaks are increasingly common in developed countries (Baker-Austin et al., 2018), partly due to rising ocean temperatures that favour the dissemination of non-cholera *Vibrio* species (temperatures exceeding 15 °C) (Baker-Austin et al., 2018; Sobrinho et al., 2010). Among the *Vibrio* genus, *V. parahaemolyticus* is a key pathogen responsible for both outbreaks and sporadic foodborne illnesses, especially related to raw or undercooked seafood consumption (Bonnin-Jusserand et al., 2019). In the USA, it is the leading cause of *Vibrio*-associated gastroenteritis, with symptoms linked to thermostable direct hemolysin (TDH) or TDH-related hemolysin (TRH) protein production (Bonnin-Jusserand et al., 2019).

Depuration is a process that reduces microorganisms in bivalves by stimulating their natural filtering activity, leading to the expulsion of intestinal contents (Pereira et al., 2021). After depuration, bivalves are deemed safe if they contain fewer than 230 most probable number (MPN) *E. coli* per 100 g of flesh and intra-valvular liquid (FIL) and are free of *Salmonella* in 25 g (European Commission, 2005, 2015). However, certain pathogens, such as *Vibrio* spp., can resist this process (Rong et al., 2014). Therefore, developing and evaluating new strategies to combat human pathogens associated with bivalve consumption is crucial (Pereira et al., 2021).

Phages, viruses that specifically infect bacteria, are increasingly used to control bacterial infections (Chhibber et al., 2008; Jun et al., 2014) and have emerged as a promising alternative for controlling pathogenic bacteria in food (Chaudhary et al., 2024). They have applications in food safety (Denes and Wiedmann, 2014; Endersen et al., 2014) as effective pathogen-killers without affecting normal microbiota (Hawkins et al., 2010; Pereira et al., 2011). Phages have also been applied to combat pathogenic bacteria associated with bivalve consumption (Duarte et al., 2021; Jun et al., 2014; Pereira et al., 2016a; Pereira et al., 2017a; Rong et al., 2014).

This study aimed to isolate and evaluate the efficacy of five new phages (PCEc3, PCST1, PCSE1, PCAh2, and PCVp3) against five bacteria relevant for human health related to bivalve consumption - *E. coli*, *S.* Typhimurium, *S.* Enteritidis, *A. hydrophila*, and *V. parahaemolyticus*.

2. Material and methods

2.1. Bacterial strains and growth conditions

The bacterial strains used in this study as phage hosts included *E. coli* (ATCC 25922), *S.* Typhimurium (ATCC 13311), *S.* Enteritidis (CVB), *A. hydrophila* (ATCC 7966) and *V. parahaemolyticus* (O22C). The bacterial strains for the host range experiment are detailed in Table S1. *Aeromonas caviae* 838, *A. hydrophila* 839 and *A. hydrophila* IR13 were isolated from Vouga River water (Tacão et al., 2015). *A. hydrophila* (ATCC 7966), *Aliivibrio fisheri* (ATCC 49387), *E. coli* (ATCC 13706 and 25922), *S.* Typhimurium (ATCC 13311 and ATCC 14028), *Vibrio parahaemolyticus* (ATCC 17802), *Aeromonas salmonicida* (CECT 894), *Vibrio alginolyticus* (CECT 521) and *V. parahaemolyticus* (DSM 27657) were purchased from the ATCC, CECT, and DSM collections. *E. coli* Scc 09, 33, 34, 35, 36, 37, 38, 40, 41, 43, 45, 47, 48, 49, 50, 51, 52, 53, 55, 56, 58, 69, 77, 78 and, 91 were isolated from an urban wastewater treatment plant (Silva et al., 2018). All *S.* Enteriditis used in this study are food sample isolates gently provided by Controlvet Laboratory. Other *Vibrio* strains used in this study were either isolated in previous research (Dias, 2020) or kindly provided by the Center of Biological Research (CIBUS) of the University of Santiago de Compostela (Galicia, Spain). The remaining bacterial strains were isolated from water samples collected in Ria de Aveiro during previous studies (Alves et al., 2008; Louvado et al., 2010; Pereira et al., 2016b).

Fresh bacterial cultures were preserved on Tryptic Soy Agar (TSA; Liofilchem, Roseto degli Abruzzi, Italy) at 4 °C. For *Vibrio* spp., TSA (Liofilchem, Roseto degli Abruzzi, Italy) was enriched with 2% NaCl (TSA-2). Before each assay, an isolated colony was aseptically transferred to Tryptic Soy Broth (TSB; Liofilchem, Roseto degli Abruzzi, Italy) or TSB enriched with 2% NaCl (TSB-2) for *Vibrio* spp., and incubated overnight at 25 °C. 100 µL of this culture were aseptically transferred to fresh TSB and incubated overnight at 25 °C until an optical density (O.D. 600 nm) of 0.8, corresponding to approximately 10^9 cells per mL, was reached.

2.2. Phage isolation and purification

PCEc3 and PCST1 were isolated in a previous study, using *E. coli* (ATCC 25922) and *S.* Typhimurium (ATCC 13311) as hosts, respectively (Costa et al., 2021). Phages PCSE1 and PCAh2 were isolated from the Aveiro's sewage network (station EEIS9 of SIMRIA Multi Sanitation System of Ria de Aveiro) using *S.* Enteritidis (CVB) and *A. hydrophila* (ATCC 7966) as hosts, respectively. Phage PCVp3 was isolated from the Aveiro River Channel water using *V. parahaemolyticus* (O22C) as the host. Sewage and river waters were filtered through 0.45 µm pore size polycarbonate membranes (Millipore, Bedford, MA, USA). The filtrate was added to a double-concentrated TSB or TSB-2 medium, along with 1 mL of fresh cultures of the respective hosts: *S.* Enteritidis (CVB), *A. hydrophila* (ATCC 7966) and *V. parahaemolyticus* (O22C). The mixtures were incubated for 18 h at 25 °C with shaking at 80 rpm, then filtered through a 0.2 µm membrane (Millipore Bedford, MA, USA). Phage concentrations were determined using the double-layer agar method (Adams, 1959), with TSA as the culture medium or TSA-2 for *Vibrio* spp. Plates were incubated at 25 °C and examined for lytic plaques after 12 h. A single plaque was isolated and transferred to TSB or TSB-2 medium containing a fresh culture of the corresponding host. The sample was then centrifuged, and the supernatant was used for a second round of phage isolation. This process involved three successive single-plaque isolation cycles to obtain pure phage stocks. Lysates were centrifuged at 10,000 × *g* for 10 min at 4 °C to remove bacterial debris, and the phage stocks were stored at 4 °C. The *S.* Enteritidis, *A. hydrophila*, and *V. parahaemolyticus* phages were designated PCSE1, PCAh2 and PCVp3, respectively. Phage titre was determined as described before, with plates incubated for 8 h at 25 °C and the number of lytic plaques counted. The results were expressed as plaque-forming units per millilitre (PFU/mL).

2.3. Phage morphological characterization via electron microscopy

Highly concentrated suspensions of three phage particles (10^9 PFU/mL) were negatively stained with 2% uranyl acetate (Electron

Microscopy Sciences, Hatfield, UK). Electron micrographs were captured using a JEOL 1011 transmission electron microscope (JEDL USA Inc., Peabody, MA, USA) operating at 100 kV. Images were acquired using a Gatan CCD-Erlangshen ES100W camera. The phages' full names were defined according to Adriaenssens and Brister (2017).

2.4. Phage DNA extraction

Phage suspensions (>10^9 PFU/mL) were centrifuged thrice at 12,000 × *g* for 10 min. Virion deoxyribonucleic acid extraction was performed in duplicate following Jakočiūnė and Moodley (2018), with bacterial RNA and DNA removal and phage capsid digestion according to Sambrook and Russel (2001). DNA purification was done using the DNeasy Blood & Tissue Kit (Qiagen, Hilden, Germany), doubling the phage lysate volume to enhance yield. DNA quantity and quality were assessed with a NanoDrop One UV-VIS spectrophotometer (Thermo Fisher Scientific, Waltham, MA, USA), following the manufacturer's protocol. For phage PCAh2 (>10^9 PFU/mL), nucleic acid extraction was conducted by SeqCenter (Pittsburgh, Pennsylvania, USA) with the ZymoBIOMICS™ DNA Miniprep Kit (Zymo Research, Irvine, California, USA) and DNA concentration was measured with a Qubit fluorometer (Thermo Fisher Scientific, Waltham, Massachusetts, USA), following the manufacturer's instructions.

2.5. Whole genome sequencing and bioinformatics analyses

The phage genomes (except for phage PCAh2) were processed for library construction using the Kapa HyperPlus kit, following the manufacturer's protocol. Genomic sequencing of the phages was conducted by Stabvida (Lisbon, Portugal) on an Illumina MiSeq platform (San Diego, California, USA) using 300 bp paired-end reads.

Quality control of the raw sequence reads was performed using FASTQC v0.11.9 (Bioinformatics Group, Babraham Institute, UK), both before and after trimming low-quality reads. Trimming was done with Trimmomatic v.0.39, applying the parameters ILLUMINACLIP: adaptors.fasta:2:30:1, Leading:8, Trailing:8, Slidingwindow:4:15, and Minlen:100 (Bolger et al., 2014). The trimmed reads were subjected to de novo genome assembly using SPAdes v.3.13.1 with the "careful" option (Bankevich et al., 2012), and the assembly graph was analysed with Bandage v0.8.1 (Wick et al., 2015). Read mapping against the resulting assembly was performed using BBMap v.38.18 to calculate the average coverage of each contig (Bushnell et al., 2017), and manual filtering was conducted to remove contigs with questionable coverage. Reads were subsequently remapped to the filtered contig set using Bowtie2 v.2.5.1 (Langmead and Salzberg, 2012) and assembled again using SPAdes v.3.13.1. Final error correction and genome polishing were carried out with Pilon v1.24 (Walker et al., 2014). Although termini prediction using PhageTerm was unsuccessful, the genomes were determined to be circularly permuted using apc.pl (https://github.com/jfass/apc), and repetitive sequence artifacts were removed. The phages genome were manually reordered based on the most closely related phage, following the method of Shen and Millard (2021).

Sequencing for phage PCAh2 was performed by SeqCenter (Pittsburgh, Pennsylvania, USA). Illumina sequencing libraries were prepared using the tagmentation- and PCR-based Illumina DNA Prep kit with custom IDT 10 bp unique dual indices (UDI), targeting an insert size of 320 bp. Sequencing was conducted on the Illumina NovaSeq 6000 platform (San Diego, California, USA) in one or more multiplexed shared-flow-cell runs, generating 2 × 151 bp paired-end reads. SeqCenter performed demultiplexing, quality control, and adapter trimming using Illumina's bcl-convert v4.1.5 software (https://support-docs.illumina.com/SW/BCL_Convert/Content/SW/FrontPages/BCL_Convert.htm) as per the manufacturer's protocol. Short-read assembly was also carried out by SeqCenter using Unicycler v0.4.8 (Wick et al., 2017).

The complete genome sequences of all phages were compared to phage genomes in GenBank using BLASTN, and the most closely related phages were identified. Genome completeness and contamination were assessed using CheckV v1.0.1 (Nayfach et al., 2021). The genome annotation was performed using Pharokka v1.3.2 (Bouras et al., 2023), with functional categorisation of CDS performed using PHROGs (Terzian et al., 2021).

2.6. Phage host range determination and efficiency of plating (EOP) analysis

The phage host range was assessed through spot testing, following the method described by Adams (1959). Plates were incubated at 25 °C and observed for plaques after 8 to 12 h. A clear lysis zone indicated bacterial sensitivity to the phage at each spot. Based on the spot's clarity, bacteria were categorised into two groups: those with clear and those without lysis zones. For bacteria that exhibited positive spot test results (clear lysis zones) (Adams, 1959), the EOP (average PFU on target bacteria/average PFU on host bacteria) (Kutter, 2009) was determined using the double-layer agar method (Adams, 1959). Three independent experiments were conducted. The EOP (Kutter, 2009) was calculated for the three measurements (Fig. 2).

2.7. Phage adsorption assay

Phage adsorption curves were determined following the methods outlined in Adams (1959) and Hyman and Abedon (2009). Exponential host bacterial cultures of *E. coli* (ATCC 25922), *S.* Typhimurium (ATCC 13311), *S.* Enteritidis (CVB), *A. hydrophila* (ATCC 7966) and *V. parahaemolyticus* (O22C) were adjusted to reach a bacterial density of 10^8 CFU/mL. Phage suspensions were added to 30 mL of each host strain to reach an MOI of 0.001 (Stuer-Lauridsen et al., 2003) and incubated at 25 °C. Aliquots of the mixtures were collected every 5 min for 15 min for phage PCEc3 and every 10 min for 40, 80, 80 and 70 min for phages PCST1, PCSE1, PCAh2 and PCVp3, respectively. The mixtures were centrifuged at 12,000 × *g* for 5 min, and unadsorbed phages were diluted and titrated. Plates were incubated at 25 °C and checked for plaques after 8 to 12 h. Adsorption was measured as the percentage decrease in phage titre in the supernatant compared to the initial measurement, with phage-only suspensions serving as a no-adsorption control (Stuer-Lauridsen et al., 2003). Three independent assays were conducted.

2.8. One-step growth curves

Exponential host bacterial cultures of *E. coli* (ATCC 25922), *S.* Typhimurium (ATCC 13311), *S.* Enteritidis (CVB), *A. hydrophila* (ATCC 7966) and *V. parahaemolyticus* (O22C) were adjusted to a density of 10^8 CFU/mL. Phage suspensions were added to 10 mL of each host strain to reach an MOI of 0.001 and incubated at 25 °C for 5 min (Mateus et al., 2014). The mixture was centrifuged at 12,000 × *g* (Thermo Heraeus Pico, Hanau, Germany) for 5 min. The resulting pellet was re-suspended in 10 mL of TSB at 25 °C, diluted until a phage density of 10^1 PFU/mL was reached and titrated by the double-layer agar method (Adams, 1959) using TSA or TSA-2 as the culture medium. Plates were incubated at 25 °C and checked for plaques after 4–8 h (Mateus et al., 2014). Three independent assays were done.

2.9. Bacterial inactivation assay

Bacterial inactivation was assessed using *E. coli* (ATCC 25922), *S.* Typhimurium (ATCC 13311), *S.* Enteritidis (CVB), *A. hydrophila* (ATCC 7966) and *V. parahaemolyticus* (O22C) as hosts at MOI of 1, 10 and 100. Each assay included two controls: a bacterial control (BC), which contained only bacteria, and a phage control (PC), which contained only phages. Both controls and test samples were incubated under identical conditions. Aliquots from the controls and test samples were collected every 2 h for 12 h and again after 24 h of incubation. Phage titres were

determined in triplicate using the drop plate method in double-layered agar (Adams, 1959) after an 8- to 12-hour incubation at 25 °C. Bacterial concentrations were assessed in triplicate for the bacterial control using the drop plate method in TSA and in duplicate for test samples using the pour plating method in TSA after a 24-hour incubation at 25 °C. Three independent experiments were conducted for each condition.

2.10. Statistical analysis

Statistical analysis was conducted using GraphPad Prism software 9 (San Diego, California, USA). The normality of the data was assessed with the Kolmogorov–Smirnov test, while Levene's test was employed to confirm the homogeneity of variance. Two-way ANOVA with repeated measures, followed by Tukey's multiple comparison post-hoc test, was utilised to evaluate significant differences between bacterial and viral concentrations (see Section 3.7). Additionally, two-way ANOVA was applied to determine whether the growth curves of the test groups differed significantly from those of the control groups (Section 3.7). A p-value of <0.05 was considered statistically significant.

3. Results

3.1. Phage isolation and purification

Phages PCEc3, PCST1, PCSE1 and PCAh2 were isolated from the Aveiro municipal sewage using *E. coli* (ATCC 25922), *S.* Typhimurium (ATCC 13311), *S.* Enteritidis (CVB) and *A. hydrophila* (ATCC 7966) as hosts, respectively. Phage PCVp3 was isolated from the Aveiro River Channel using *V. parahaemolyticus* (O22C) as the host. Phages PCEc3, PCST1, PCSE1, PCAh2 and PCVp3 formed clear plaques on the host strain with diameters of 4.0–9.0, 2.0-4.0, 0.5-1.0, 1.0-2.0 and 1.0-1.5 mm, respectively, after 12 h of incubation at 25 °C (Fig. 1). High titre suspensions ($>10^{10}$ PFU/mL) were achieved for all phages.

3.2. Virion morphology

Based on morphological analysis using Transmission Electron Microscopy (TEM) (Fig. S1), all phages were classified as members of the Caudoviricetes Class. Phage PCEc3 exhibits a siphovirus morphotype with an icosahedral head measuring approximately 60.1 ± 0.7 nm in width and a long, flexible tail approximately 200 nm long. Similarly, phage PCST1 showcases a siphovirus morphotype with an icosahedral head width of approximately 56.5 ± 1.5 nm and a long, flexible tail approximately 200 nm long. Phage PCSE1 features a myovirus morphotype with an icosahedral head with a width of approximately 71.47 ± 4.55 nm and a long, retractive tail measuring approximately 121.88 ± 3.40 nm in length. Phage PCAh2 features a myovirus morphotype with an icosahedral head with a width of approximately 58.75 ± 1.25 nm and a long, retractive tail measuring approximately 134 ± 20 nm. Phage PCVp3 features a siphovirus morphotype with an icosahedral head with a width of approximately 61.12 ± 11.11 nm and a long tail measuring approximately 133 ± 11 nm.

3.3. Genomic features and analysis

The genome of phages PCEc3 (GenBank: PQ314493), PCST1 (GenBank: PQ374047), PCSE1 (GenBank: PQ314491), PCAh2 (GenBank: PQ314494) and PCVp3 (GenBank: PQ314492) were sequenced as described above (Section 2.5). These phages possess double-stranded DNA genomes, with their genomic features (Fig. 1) summarised in Table 1 and detailed in Tables S2-S6. Our analysis did not detect genes encoding antibiotic resistance or virulence factors across all phage genomes. The absence of known integrase genes suggests that all phages could be viable candidates for biocontrol applications. However, a CII-like transcriptional activator gene was identified in phage PCAh2, which may indicate lysogenic potential (Table S5). Additionally, tRNA genes were detected in the genome of phage PCEc3, implying that the phage might rely on its tRNA for translation post-infection (Fig. 1, Table S2). Overall, we identified putative genes encoding proteins associated with DNA modification and replication, packaging and structural components, and host lysis mechanisms (e.g., holin and endolysin) (Fig. 1, Tables S2–S6).

3.4. Analysis of phage host range and efficiency of plating (EOP)

Spot tests revealed that phages PCEc3, PCST1, PCSE1, and PCAh2 displayed completely cleared zones on 4, 7, 7 and 7 of the 57 strains tested, respectively, and PCVp3 could only form a completely cleared zone on its host (Tables 2, A1).

However, EOP results (Fig. 2) indicate that the phage PCEc3 formed lysis plaques only in the presence of its host. In addition to its host, phage PCST1 formed lysis plaques on *E. coli* ATCC 25922 and *E. coli* Scc 34. Similarly, phage PCSE1, besides its host, formed lysis plaques on *S.* Enteritidis CVA and *E. coli* ATCC 25922. Phage PCAh2, apart from its host, formed lysis plaques on *A. hydrophila* 839, *E. coli* ATCC 25922 and *S.* Typhimurium ATCC 13311.

3.5. Phage adsorption

Phage adsorption assays revealed that approximately 87% of phage PCEc3 particles adsorbed to *E. coli* within 5 min, increasing to 95 % after 15 min (Fig. 3A). For phage PCST1, 50% of phage particles were adsorbed to *S.* Typhimurium within 20 min and 59% after 40 min (Fig. 3B). For phage PCSE1, 50% of phage particles were adsorbed to *S.* Enteritidis within 10 min and 98% after 80 min (Fig. 3C). For phage PCAh2, 19% of phage particles were adsorbed to *A. hydrophila* within 20 min and 24% after 60 min (Fig. 3D). Furthermore, for phage PCVp3, 50% of phage particles were adsorbed to *V. parahaemolyticus* within 10 min and 99% after 70 min (Fig. 3E).

3.6. One-step growth curves

One-step growth curves for all phages were established in TSB at 25 °C (Fig. 4). Analysis of the triphasic curves yielded the following results: phage PCEc3 had a latent period of 10 min and a burst size of 42.59 ± 8.66 PFU/host cell (Fig. 4A); phage PCST1 exhibited a latent period of 10 min and a burst size of 22.21 ± 5.59 PFU/host cell (Fig. 4B); for phage PCSE1, the latent period was 120 min, and a burst size reached 83.97 ± 39.21 PFU/host cell (Fig. 4C); phage PCAh2 displayed a latent period of 70 min and a burst size of 7.60 ± 3.04 PFU/host cell (Fig. 4D); lastly, phage PCVp3 had a latent period of 60 min, with a burst size of 9.16 ± 1.57 PFU/host cell (Fig. 4E).

3.7. Killing curves

The bacterial kill curves for all five phages were conducted in TSB at 25 °C with their respective hosts. Three different MOIs were used to assess potential variations in bacterial inactivation with differing phage concentrations.

Across all assays, the bacterial density in the control group (BC) increased by 2.93 to 3.57 log CFU/mL after 24 h of incubation (ANOVA, $p < 0.05$, Fig. 5A1–E1).

When challenged with phage PCEc3 at MOIs 1, 10, and 100, *E. coli* displayed similar inactivation profiles, achieving maximum bacterial reductions of 4.61, 4.59, and 4.75 log CFU/mL, relative to the bacterial control after 6 h of incubation, respectively (ANOVA, $p < 0.05$, Fig. 5A1). Notably, although inactivation started after 2 h for all MOIs, MOI 100 exhibited tenfold greater efficacy than MOI 1 (ANOVA, $p < 0.05$, Fig. 5A1).

In the case of *S.* Typhimurium challenged with phage PCST1 at MOIs 10 and 100, comparable inactivation patterns were observed, achieving

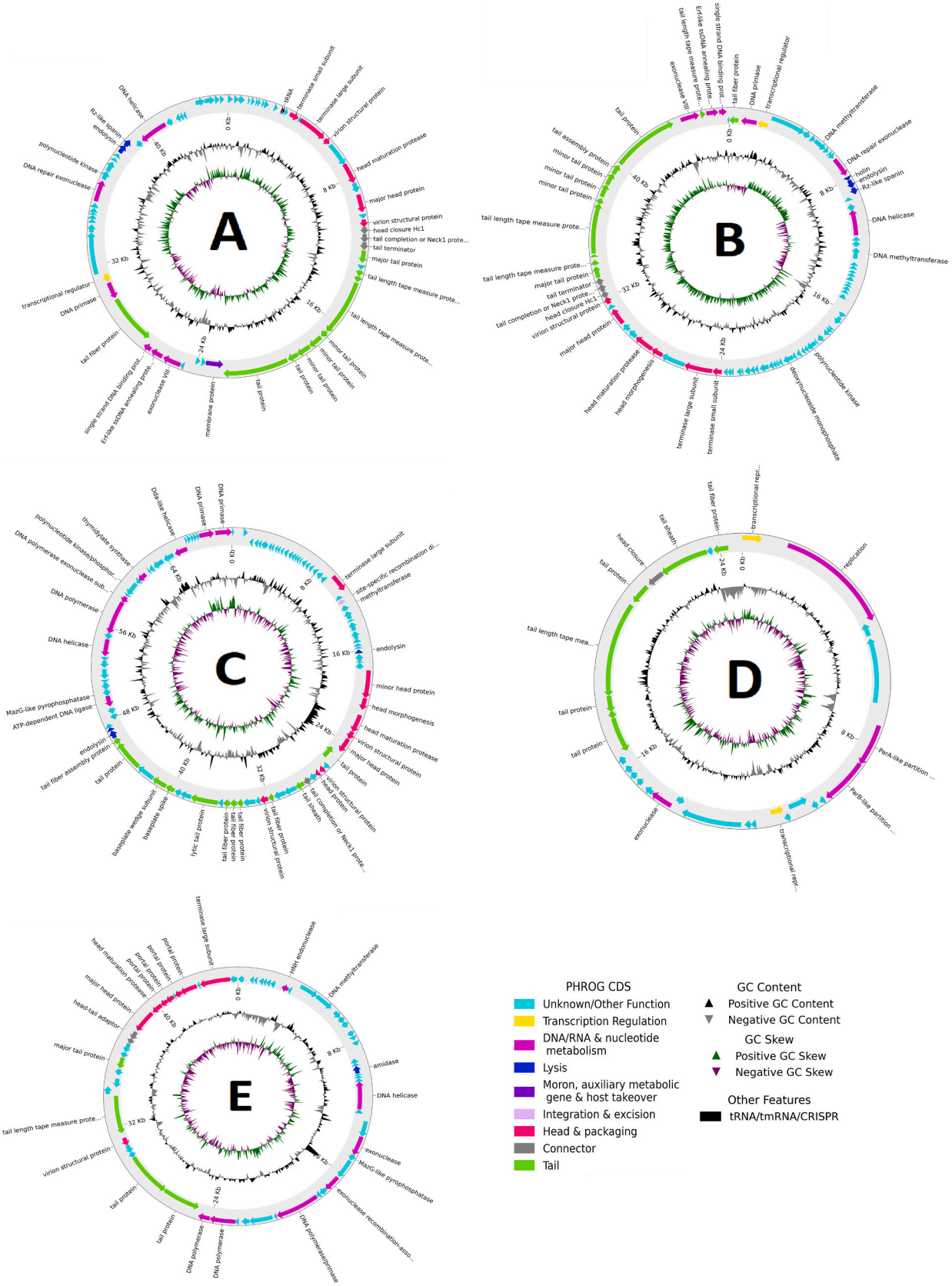

Fig. 1. Genome map of phages PCEc3 (A), PCST1 (B), PCSE1 (C), PCAh2 (D) and PCVp3 (E). The outermost circle, represented by arrow-shaped bands, illustrates the coding DNA sequences (CDS), colour-coded by functional category, aligned with the direction of transcription. The innermost ring displays the GC skew (green/pink), followed by the GC content (black/grey). Labels indicate the predicted functions of the CDS, color-coded according to the PHROGs functional categories.

Table 1
Phages' genomic features.

Full name	vB_EcoS_UALMA_PCEc3	vB_SeTS_UALMA_PCST1	vB_SeEM_UALMA_PCSE1	vB_AhyM_UALMA_PCAh2	vB_VpaS_UALMA_PCVp3
Short name	PCEc3	PCST1	PCSE1	PCAh2	PCVp3
Host	*Escherichia coli* ATCC 25922	*Salmonella enterica* serovar Typhimurium ATCC 13311	*Salmonella enterica* serovar Enteritidis CVB	*Aeromonas hydrophila* ATCC 7966	*Vibrio parahaemolyticus* O22C
Class	Caudoviricetes				
Genome size (bp)	44,679	49,364	69,920	45,282	45,076
GC content (%)	44.42	42.91	45.23	57.8	43.54
Completeness (%)	96.44	93.6[a]	100	95.42	100
Contamination (%)	0	0	0	0	0
Best Blast hit (query coverage, identity)	*Escherichia* phage vB_Ecos_CEB_EC3a (90%, 92.91%)	*Salmonella* phage phSE-5 (96%, 99.24%)	No hit	*Aeromonas* phage phiARM81ld (83%, 87%)	No hit
Number of CDS	68	85	100	57	63
Number of hypothetical proteins	38 (56%)	50 (59%)	64 (64%)	26 (46%)	39 (62%)
Number of functional proteins	30 (44%)	35 (41%)	36 (36%)	31 (54%)	24 (38%)
tRNA genes	2	0	0	0	0
PhageTerm	Undetermined	Headful (pac) P1	Headful (pac) P1	Undetermined	COS (3′)

[a] The genome consists of 3 contigs—value only of the largest contig.

Table 2
Phages host range with apparent lysis.

Bacterial Strains	PCEc3	PCST1	PCSE1	PCAh2	PCVp3
Aeromonas hydrophila 839	X	X	X	●	ND
Aeromonas hydrophila ATCC 7966	X	X	X	●	X
Escherichia coli ATCC 25922	●	●	●	●	X
Escherichia coli Scc 34	X	●	X	●	ND
Escherichia coli Scc 40	●	●	●	●	ND
Escherichia coli Scc 69	X	●	X	X	ND
Salmonella enterica serovar Enteriditis CVA	X	X	●	X	ND
Salmonella enterica serovar Enteriditis CVB	X	●	●	X	X
Salmonella enterica serovar Enteriditis CVD	●	●	●	●	ND
Salmonella enterica serovar Typhimurium ATCC 13311	●	●	●	●	X
Vibrio parahaemolyticus 022C	X	X	X	X	●
Vibrio parahaemolyticus DSM 27657	X	X	●	X	X

Note: The full table is displayed in Table S1.
ND – not determined.
● – clear lysis zone.
X – no lysis zone.

maximum bacterial reductions of 3.71 and 3.56 log CFU/mL, relative to the bacterial control after 10 h of incubation (ANOVA, $p < 0.05$, Fig. 5B1), respectively. Both MOIs initiated inactivation after 2 h, with MOI 100 showing greater efficacy than MOI 10 (ANOVA, $p < 0.05$, Fig. 5B1). However, at MOI 1, inactivation began after 4 h and reached its maximum (3.73 log CFU/mL) after 10 h of incubation (ANOVA, $p < 0.05$).

Similarly, when challenged with phage PCSE1 at MOIs 10 and 100, *S.* Enteritidis demonstrated inactivation after 2 h of incubation. However, their maximum bacterial reductions (4.34 and 4.23 log CFU/mL, respectively), relative to the bacterial control, were achieved at different times, after 6 and 8 h of incubation, respectively (ANOVA, $p < 0.05$, Fig. 5C1). At MOI 1, inactivation started after 4 h, reaching its peak (4.03 log CFU/mL) after 8 h of incubation (ANOVA, $p < 0.05$).

For *A. hydrophila* challenged with phage PCAh2 at MOIs 10 and 100, inactivation started after 2 h, with maximum reductions (4.57 and 4.00 log CFU/mL, respectively), relative to the bacterial control, observed after 8 h (ANOVA, $p < 0.05$, Fig. 5D1). At MOI 1, inactivation started after 6 h, achieving a higher peak (5.57 log CFU/mL) after 8 h of incubation (ANOVA, $p < 0.05$).

Lastly, when challenged with phage PCVp3 at MOIs 10 and 100, *V. parahaemolyticus* displayed inactivation beginning after 2 h, reaching maximum reductions (4.33 and 4.46 log CFU/mL, respectively), relative to the bacterial control, after 6 h of incubation (ANOVA, $p < 0.05$, Fig. 5E1). At MOI 1, inactivation began and reached its maximum (0.80 log CFU/mL) after 2 h of incubation. From 4 h onward, no significant differences were observed compared to the control (Fig. 5E1; ANOVA, $p > 0.05$).

All phage controls (PC) maintained stability throughout the 24-hour experiments (ANOVA, $p > 0.05$, Fig. 5A2–E2).

In the presence of their hosts, all phages (except phage PCVp3) showed an increase in their survival factor at MOIs of 1 and 10 after 2 to 6 h of incubation, with approximately 10- to 1000-fold increases in phage titres after 24 h (ANOVA, $p < 0.05$, Fig. 5A2–E2). At an MOI of 100, phage titre increases were observed only after 24 h of incubation (ANOVA, $p < 0.05$, Fig. 5A2–E2).

Phage PCVp3, at an MOI of 1, displayed a continuous decrease in its survival factor after 4 h of incubation, resulting in a 4.34 log PFU/mL titre after 24 h, representing a 100-fold reduction. At MOIs 10 and 100, the phage titre remained stable, comparable to the control, with only a slight increase observed at MOI 10 after 24 h (0.40 log PFU/mL [Fig. 5A2–E2]; ANOVA, $p < 0.05$).

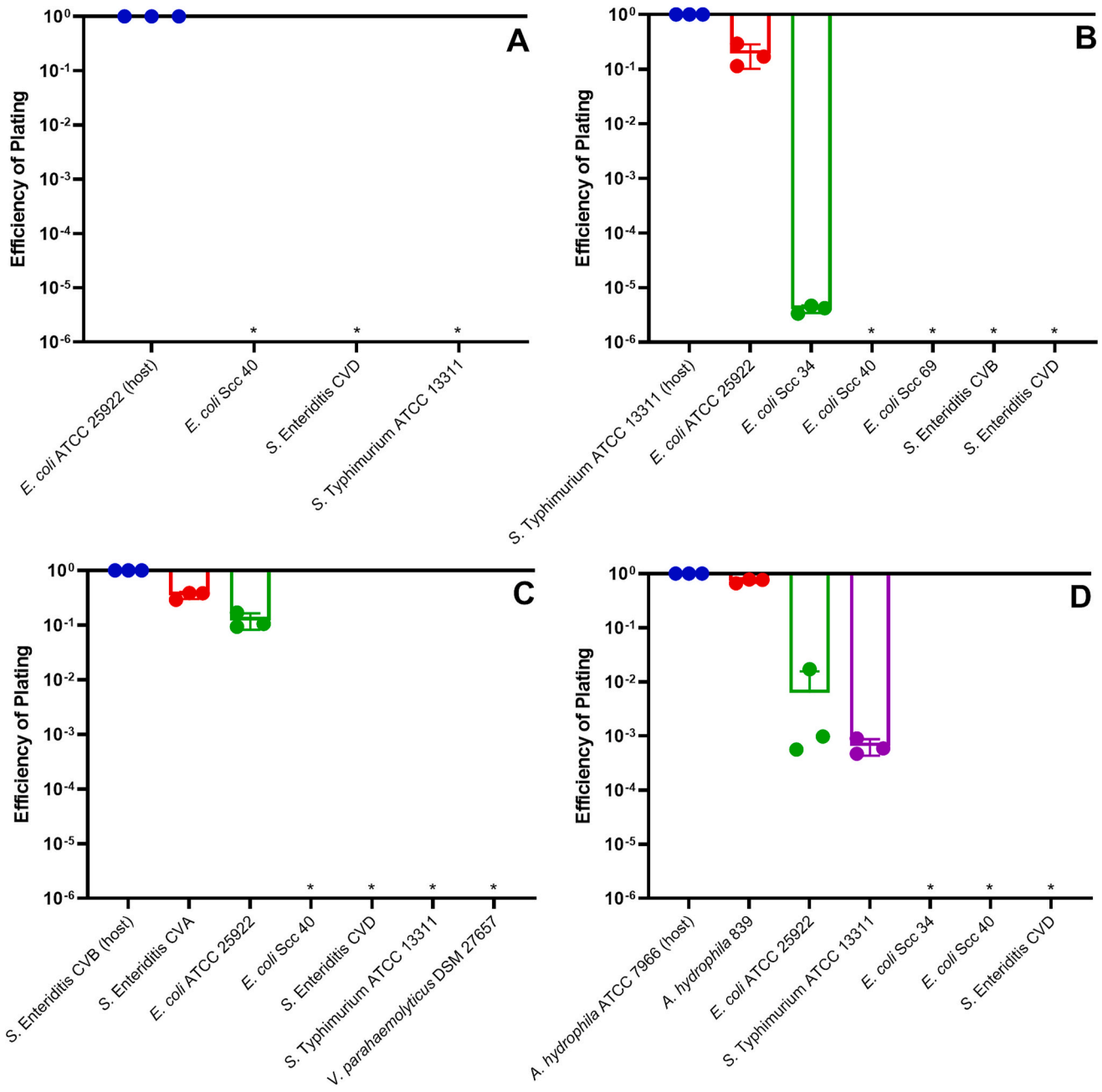

Fig. 2. Efficiency of plating of *E. coli* phage PCEc3 (A), *S.* Typhimurium phage PCST1 (B), *S.* Enteritidis phage PCSE1 (C) and *A. hydrophila* phage PCAh2 (D). *No phage lysis plaques detected.

4. Discussion

Bivalves, crucial to the human diet and increasingly valuable commercially (FAO, 2024), filter particles and pathogens from seawater, posing health risks when consumed raw or undercooked (Pereira et al., 2021; Zannella et al., 2017). While depuration, a widely used process to eliminate microorganisms, is effective in many cases (Pereira et al., 2021), pathogens like *Vibrio* spp. often resist this method, posing persistent risks (Martínez et al., 2009; Rong et al., 2014). Phages have emerged as a promising alternative for controlling pathogenic bacteria in food (Chaudhary et al., 2024) due to their proven applications in food safety (Denes and Wiedmann, 2014; Endersen et al., 2014) and their effectiveness in managing bacteria associated with bivalve consumption (Duarte et al., 2021; Jun et al., 2014; Pereira et al., 2016a; Pereira et al., 2017a; Rong et al., 2014). Selecting suitable phages for biocontrol requires careful evaluation of factors including host range, adsorption rate, latent period, burst size, lysogenic potential, and safety (Mateus et al., 2014; Pereira et al., 2011).

Different plaque sizes were observed for the isolated phages, with diameter ranging between 0.5 and 9.0 mm (Fig. S1). Although plaque size in semi-solid media is sometimes linked to lysis rates in liquid bacterial suspensions (Ameh et al., 2020), this study found no consistent correlation. For instance, while phage PCEc3, with the largest plaques (4–9 mm) (Fig. S1A), exhibited the fastest bacterial inactivation (Fig. 5A), followed by phages that produced medium to small plaques (0.5 to 4.0 mm) (Fig. S1B–E), phage PCSE1, which produced the smallest plaques, presented a lysis rate similar to phage PCST1, which formed medium-sized plaques. Variations in bacterial density, diffusion, and metabolic activity between agar and liquid environments (Abedon and Yin, 2009), likely contribute to these discrepancies. While plaque size is

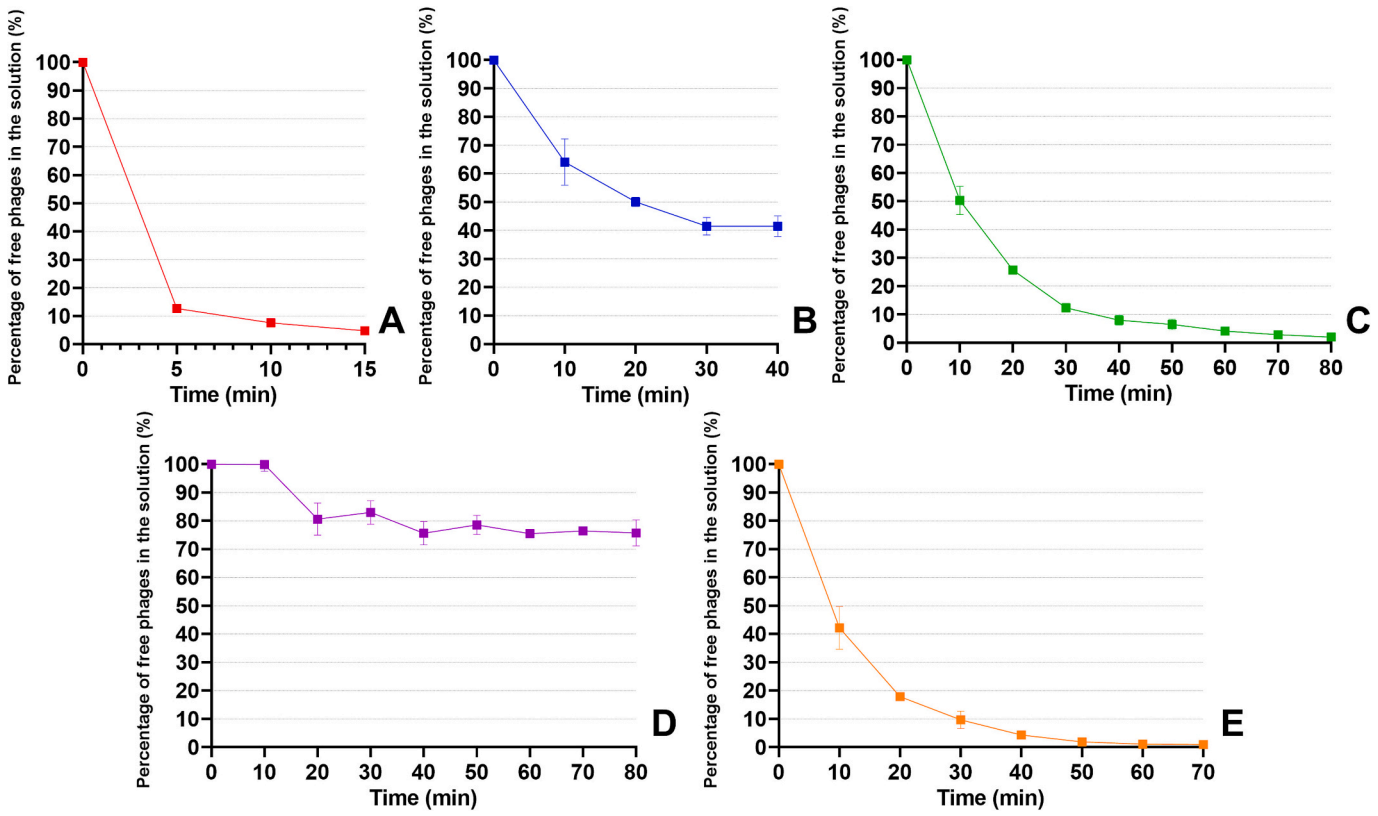

Fig. 3. Adsorption curves of phages PCEc3 (A), PCST1 (B), PCSE1 (C), PCAh2 (D) and PCVp3 (E) in the presence of their hosts *E. coli*, *S.* Typhimurium and *S.* Enteritidis, *A. hydrophila* and *V. parahaemolyticus*, respectively. The percentage of unadsorbed phage was calculated as the ratio of PFU in the supernatant to the initial PFU, using equivalent dilutions of the phage without host cells as a reference. Values represent the mean of three independent experiments, with error bars indicating the standard deviation.

influenced by factors such as burst size and adsorption rate (Gallet et al., 2011), its relevance for selecting biocontrol phages remains debated (Ameh et al., 2020).

Phage PCEc3 plaques stood out by their size and morphology, characterized by a central core and a wide halo (Fig. S1A). Similar wide halos, a result from the degradation of the bacterial envelope by phage enzymes (depolymerase) (Cai et al., 2019; Knecht et al., 2020), were also observed in *Serratia liquefaciens* KKP 3654 phage KKP 3708 plaques (Shymialevich et al., 2022). However, the halo size could be related to factors such as enzyme secretion, phage concentration in the plaques (Cornelissen et al., 2011), and/or phage diffusion through the agar (Cornelissen et al., 2011; Shymialevich et al., 2022).

The morphotypes observed by TEM (Fig. S1) align with the class classification suggested by genome sequencing. The genome sequences of phages PCSE1 and PCVp3 did not match any known sequences. Phage PCEc3 shows 92.91% similarity to *E. coli* phage vB_Ecos_CEB_EC3a, which infects *E. coli* Ec3a and *E. coli* ATCC 25922 and has a siphovirus morphotype (Oliveira et al., 2018). Phage PCST1 has a 99.24% similarity with *S.* Typhimurium phage phSE-5, which also has *S.* Typhimurium ATCC 13311 as a host and has a siphovirus morphotype (Pereira et al., 2016a). Phage PCAh2 shares 87% similarity with *Aeromonas* sp. ARM81 phage ΦARM81ld, a chemically activated (mitomycin C 500 μg/mL) prophage with a myovirus morphotype (Dziewit and Radlinska, 2016). Genomic analysis of the phages revealed no known genes encoding antibiotic resistance, toxins, or integrase enzymes, indicating their safety for phage biocontrol. While four of the five tested phages are likely lytic—a key requirement for biocontrol—phage PCAh2 may possess lysogenic potential due to the presence of a gene encoding a CII-like transcriptional activator (Table S4)—a protein crucial for initiating the lysogenic life cycle (Lamont et al., 1993; Neufing et al., 2001) — and analysis by the PhageAI S.A. program, which predicts an 80.84% likelihood of lysogeny. While no known integrase genes, which are essential for lysogeny establishment (Fogg et al., 2011), were detected in phage PCAh2, further studies are needed to confirm any potential lysogenic capability. Strictly lytic phages are recommended for biocontrol applications to prevent potential transfer of antibiotic resistance or virulence genes (Harrison and Brockhurst, 2017; Oliveira et al., 2015). However, advancements in phage genome engineering (Monteiro et al., 2019; Zhou et al., 2023) have enabled the modification of temperate phages to improve safety and efficacy (Łobocka et al., 2021; Monteiro et al., 2019). Despite containing a lysogenic-related gene (Table S4), phage PCAh2 demonstrated high host inactivation efficiency, achieving maximum reductions of 4.00 to 5.57 log CFU/mL (Fig. 5D). Thus, future studies should explore genome engineering to remove lysogeny-related genes, enhancing phage PCAh2's safety while maintaining its inactivation efficiency.

Four of the five phages tested formed cleared zones on 4 to 7 of the 57 strains, with phage PCVp3 exhibiting a very narrow host range by forming a clear zone only on its host (Table 2). However, EOP results indicate that most phages could only infect two other strains besides their original host (Fig. 2). Specifically, phages PCST1, PCSE1, and PCAh2 each infected three strains (Fig. 2). Similar observations by Mirzaei and Nilsson (2015) and Pereira et al. (2017b) suggest that spot tests alone may not reliably assess phage infectivity, highlighting the need for EOP assays. Lysis from without is a plausible mechanism that occurs when bacterial cells are overwhelmed by phages, leading to rupture through lysin activity or rapid depletion of cellular resources (Abedon, 2011). Host range depends on the interaction between phage tail fibers and host cell receptors (Endersen et al., 2014; Hanlon, 2007), and modifications to these structures can alter host specificity (Pereira et al., 2017a). Most of the isolated phages were able to infect the host of another phage, indicating their potential use in phage cocktails (Costa

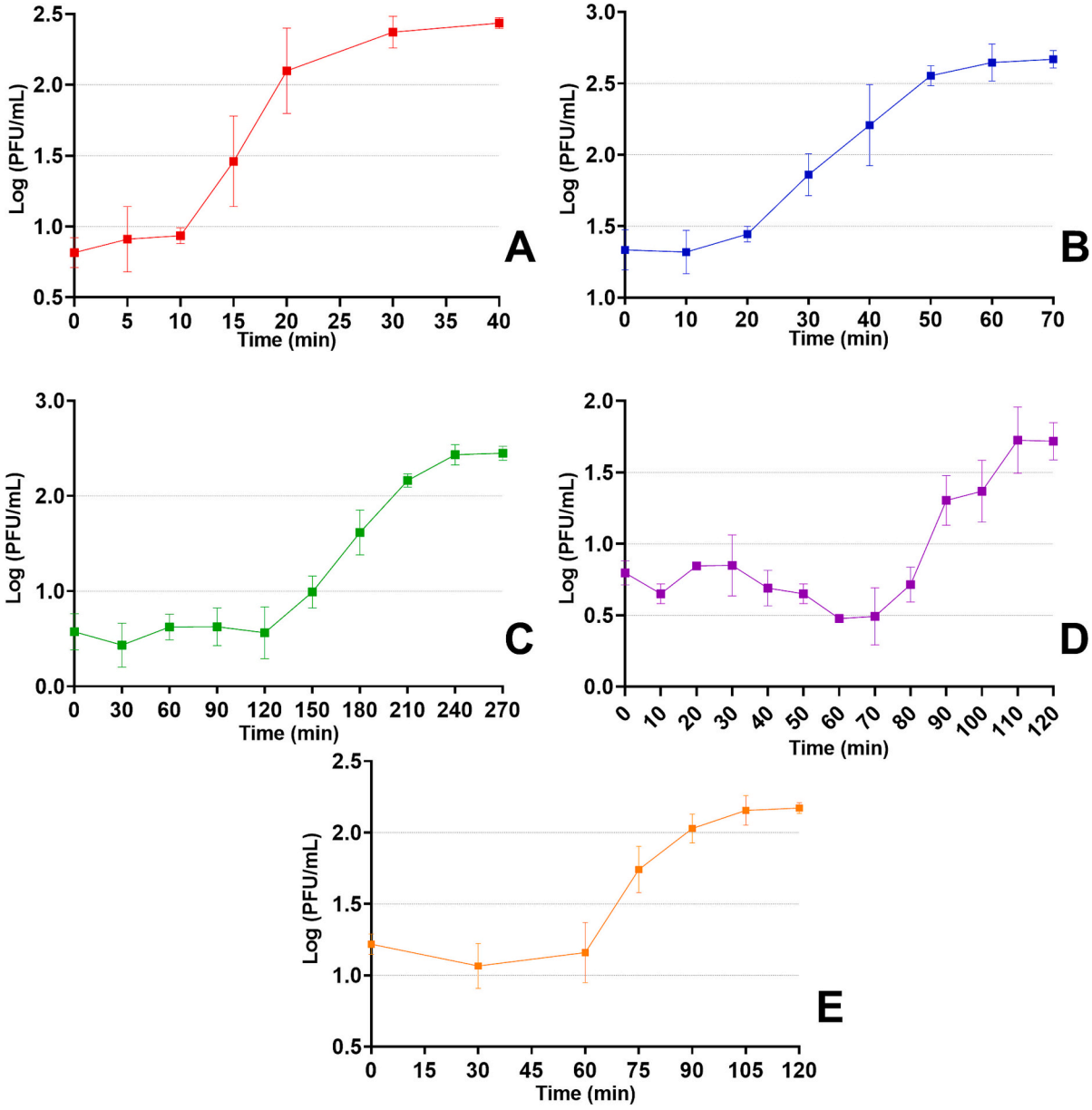

Fig. 4. One-step growth curves of phages PCEc3 (A), PCST1 (B), PCSE1 (C), PCAh2 (D) and PCVp3 (E) in the presence of their hosts *E. coli*, *S.* Typhimurium, *S.* Enteritidis, *A. hydrophila* and *V. parahaemolyticus*, respectively. Values represent the mean of three independent experiments, with error bars indicating the standard deviation.

et al., 2019). However, further studies are needed to understand the dynamics between these phages when combined in a cocktail.

Adsorption is the initial step in phage infection, involving the specific binding of bacteriophages to bacterial surface receptors (Ge et al., 2020) and is a crucial determinant of infection dynamics (Hurley et al., 2008; Rodin and Ratner, 1983). Understanding the molecular mechanisms of the phage adsorption process is essential (Dimitrov, 2004; Skehel and Wiley, 2000) for ensuring safe and efficient phage application (Ge et al., 2020). In this study, adsorption was highly efficient for most phages, ranging between 95% and 99% (Fig. 3). However, phages PCST1 and PCAh2 showed lower adsorption efficiency, with total adsorption of 59% in 40 min (Fig. 3B) and 24% in 60 min (Fig. 3D), respectively. These reduced efficiencies may stem from changes in bacterial physiology (Igler, 2022), gene expression triggered by phage-lysed products (Bull et al., 2014; Li et al., 1961), environmental factors, or inherent variability within bacterial populations (Bull et al., 2014). Variability in adsorption could also reflect differences in the phage population (Storms et al., 2012; Storms and Sauvageau, 2015), particularly variations in the number of tail fibers, which are critical for attachment (Bull et al., 2014). The mechanisms underlying the reduced adsorption of *S.* Typhimurium phage PCST1 and *A. hydrophila* phage PCAh2 remain unclear, warranting further investigation once their receptors are identified.

Phage latent period and burst size are critical factors in selecting phages (Pereira et al., 2016a) for biocontrol applications. A one-step growth curve was conducted to assess the latent period—the time required for phage replication—and the burst size, which refers to the number of phages released per infected host (Guzel et al., 2024). All phages exhibited burst sizes similar to those reported in other studies for *E. coli* (Litt et al., 2018; Salim et al., 2022), *S.* Typhimurium (Pereira et al., 2016a; Wong et al., 2014), *S.* Enteritidis (Ahmadi et al., 2016; Li et al., 2020), *Aeromonas* (Vincent et al., 2017) and *V. parahaemolyticus* (Tan et al., 2021; Ye et al., 2022) phages. Phages PCEc3 and PCST1 displayed short latent periods of approximately 10 min (Fig. 4A, B), akin

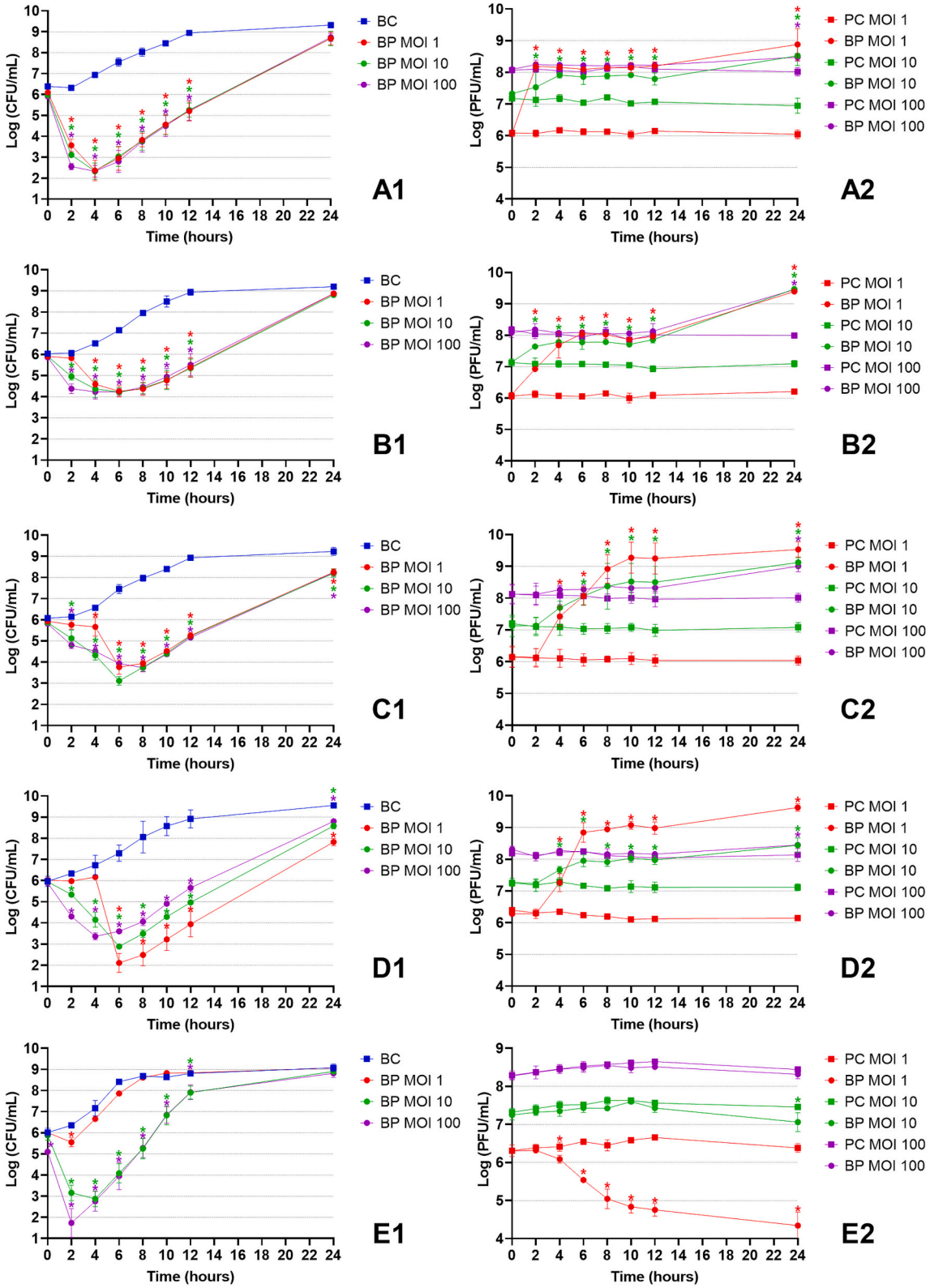

Fig. 5. Inactivation of *E. coli* (A), *S.* Typhimurium (B), *S.* Enteritidis (C), *A. hydrophila* (D) and *V. parahaemolyticus* (E) using phages PCEc3 (A), PCST1 (B), PCSE1 (C), PCAh2 (D) and PCVp3 (E), respectively, at three different MOIs. 1) Bacterial concentrations: BC – Bacterial control; BP MOI 1 – Bacteria with phage at an MOI of 1; BP MOI 10 – Bacteria with phage at an MOI of 10; BP MOI 100 – Bacteria with phage at an MOI of 100. (2) Phage concentration: PC MOI 1 – phage control at an MOI of 1; PC MOI 10: phage control at an MOI of 10; PC MOI 100: phage control at an MOI of 10; BP MOI 1 - Bacteria with phage at an MOI of 1; BP MOI 10 - Bacteria with phage at an MOI of 10; BP MOI 100 – Bacteria with phage at an MOI of 100. The values represent the mean of three independent experiments, with error bars indicating standard deviation; *$p < 0.05$ compared to the respective control.

to those observed in other *E. coli* (Salim et al., 2022; Zhou et al., 2022) and *S.* Typhimurium phages (Sun et al., 2022; Zhang et al., 2024a) phages. In contrast, phages PCAh2 and PCVp3 exhibited longer latent periods (60–70 min) (Fig. 4D, E), like those found in other *A. hydrophila* (Rai et al., 2023) and *V. parahaemolyticus* (Xu et al., 2023; Zhang et al., 2024b) phages. Phage PCSE1 exhibited an exceptionally long latent period of 120 min (Fig. 4C), which, to our knowledge, is the longest reported for a *S.* Enteritidis phage. While the latent periods for *S.* Enteritidis phages are around 30 min (Dallal et al., 2019; Guzel et al., 2024; Sobhy et al., 2021), longer latent periods (142 to 150 min) have been reported in other *Myoviridae* phages (Vincent et al., 2017).

Understanding *in vitro* phage-host replication dynamics is essential for effective biocontrol of pathogenic bacteria. The kinetic theory of phage application suggests that MOI could significantly influence bacterial inactivation efficiency (Pereira et al., 2017a) and play a key role in prospective phage applications (Ssekatawa et al., 2021). In this study, phages PCEc3, PCST1, and PCSE1 demonstrated similar inactivation efficiency and maximum bacterial reductions across different MOI values (Fig. 5). In contrast, phages PCAh2 and PCVp3 showed differing outcomes at MOI 1: PCAh2 achieved a maximum reduction of 5.57 log CFU/mL after 8 h (Fig. 5D), whereas PCVp3 exhibited low inactivation, with a maximum reduction of 0.80 log CFU/mL after 2 h (Fig. 5E). For all phages, higher MOIs led to faster inactivation rates, as increased MOI enhances the likelihood of phage particles infecting their host bacteria (Artawinata et al., 2023; Ssekatawa et al., 2021). Phage PCEc3 achieved the fastest inactivation within 2 h across all MOIs (Fig. 5A), likely due to its rapid adsorption rate (95% in 15 min) and short latent period (10 min). In contrast, slower inactivation rates observed at lower MOIs in other phages could be attributed to longer adsorption rates (98-99% in 70 to 80 min; Fig. 3C, E), extended latent periods (60 to 120 min; Fig. 4C, E), or inefficient adsorption (24% in 60 min; Fig. 3D) combined with long latent periods (70 min; Fig. 4D). Although inactivation rates were generally slower at MOI 1, the maximum inactivation achieved was similar in magnitude and timing to that observed at higher MOIs (Fig. 5A1–E1). This inactivation was also accompanied by a greater increase in phage concentration than at the higher MOIs (Fig. 5A2–E2), supporting the hypothesis that precise initial phage doses may not be essential due to the phage's self-perpetuating nature (Nakai, 2010; Payne and Jansen, 2003).

Conversely, phage PCVp3 concentration decreased at MOI 1 in the presence of the host (Fig. 5E2), which could be attributed to the absence of $CaCl_2$ and $MgSO_4$ in the TSB broth (Bryner et al., 1970). $CaCl_2$ can stabilise the interaction between bacteria and phages (receptor and ligand) through electrostatic interactions (Adnan et al., 2020), affecting adsorption, penetration, and other stages of phage propagation (Rafiei and Bouzari, 2024). However, at higher MOI levels (10 and 100), no significant changes in phage concentration were observed during the experiment, apart from a slight increase of 0.4 PFU/mL at MOI 10 after 24 h of incubation (Fig. 5E2). Interestingly, the reduction in phage PCVp3 concentration at MOI 1 occurs after 4 h in the presence of the host, despite its lytic cycle—including adsorption and burst size—being completed within 2 h (Figs. 3E and 4E). This could suggest that bacterial defence mechanisms, such as restriction-modification systems, CRISPR, or abortive infection systems (Costa et al., 2024), may be triggered by prolonged phage-host interactions, leading to phage destruction. Further studies are needed to elucidate the mechanisms responsible for this reduction and to assess their implications for future phage applications.

5. Conclusion

The results of this study suggest that phage biocontrol can be an effective alternative to combat pathogenic bacteria associated with bivalve consumption. Although the phages exhibited different burst sizes and latent periods, they could inactivate their respective hosts effectively. While one phage might be lysogenic, steps can be taken to mitigate potential adverse effects, or a safer phage could be isolated. The demonstrated bacterial inactivation efficiency, coupled with the safety profile of these phages, paves the way for more in-depth studies, particularly *in vivo* studies, regarding the potential control of pathogenic bacteria in bivalves.

Supplementary data to this article can be found online at https://doi.org/10.1016/j.ijfoodmicro.2025.111096.

CRediT authorship contribution statement

Pedro Costa: Writing – original draft, Visualization, Investigation, Formal analysis, Data curation, Conceptualization. **Carla Pereira:** Writing – review & editing, Visualization, Validation, Supervision, Conceptualization. **Vanessa Oliveira:** Writing – review & editing, Visualization, Formal analysis, Data curation. **Newton C.M. Gomes:** Writing – review & editing, Visualization, Formal analysis, Data curation. **Jesús L. Romalde:** Writing – review & editing, Visualization, Validation, Supervision, Resources, Funding acquisition, Conceptualization. **Adelaide Almeida:** Writing – review & editing, Visualization, Validation, Supervision, Resources, Funding acquisition, Conceptualization.

Consent for publication

Not applicable.

Ethics approval and consent to participate

Not applicable.

Declaration of Generative AI and AI-assisted technologies in the writing process

While preparing this work, the authors used OpenAI's ChatGPT and Grammarly AI to check grammar and improve readability and language. After using these tools/services, the authors reviewed and edited the content as needed and take full responsibility for the publication's content.

Funding

Through national funds, we acknowledge financial support to CESAM by FCT/MCTES (UIDP/50017/2020+UIDB/50017/2020+LA/P/0094/2020).

Declaration of competing interest

The authors declare that the research was conducted without any commercial or financial relationships that could potentially create a conflict of interest.

Acknowledgements

Thanks to the Department of Biology and the University of Aveiro, where this research was carried out. The authors are also grateful to CESAM and its funding sources. Pedro Costa was supported in the form of a PhD grant (PD/BD/150360/2019) and Carla Pereira by a Junior Research contract (DOI: 10.54499/CEECIND/03974/2017/CP1459/CT0022), financed by national funds through the FCT - Foundation for Science and Technology, I.P. Vanessa Oliveira was funded by National funds (OE), through FCT, IP., in the scope of the framework contract foreseen in the numbers 4, 5 and 6 of article 23 of the Decree-Law 57/2016, of August 29, changed by Law 57/2017, of July 19 (DOI 10.54499/DL57/2016/CP1482/CT0109).

Data availability

The data underlying this article are available in the article and in its online supplementary material.

References

Abedon, S., 2011. Lysis from without. Bacteriophage 1, 46–49.
Abedon, S.T., Yin, J., 2009. Bacteriophage Plaques: Theory and Analysis, pp. 161–174.
Adams, M., 1959. Bacteriophages (New York).
Adnan, M., Ali Shah, M.R., Jamal, M., Jalil, F., Andleeb, S., Nawaz, M.A., Pervez, S., Hussain, T., Shah, I., Imran, M., Kamil, A., 2020. Isolation and characterization of bacteriophage to control multidrug-resistant *Pseudomonas aeruginosa* planktonic cells and biofilm. Biologicals 63, 89–96.
Adriaenssens, E., Brister, J.R., 2017. How to name and classify your phage: an informal guide. Viruses 9, 70.
Ahmadi, M., Karimi Torshizi, M.A., Rahimi, S., Dennehy, J.J., 2016. Prophylactic bacteriophage administration more effective than post-infection administration in reducing *Salmonella enterica* serovar Enteritidis shedding in quail. Front. Microbiol. 7.
Alves, E., Carvalho, C.M.B., Tomé, J.P.C., Faustino, M.A.F., Neves, M.G.P.M.S., Tomé, A. C., Cavaleiro, J.A.S., Cunha, Â., Mendo, S., Almeida, A., 2008. Photodynamic inactivation of recombinant bioluminescent *Escherichia coli* by cationic porphyrins under artificial and solar irradiation. J. Ind. Microbiol. Biotechnol. 35, 1447–1454.
Ameh, E.M., Tyrrel, S., Harris, J.A., Pawlett, M., Orlova, E.V., Ignatiou, A., Nocker, A., 2020. Lysis performance of bacteriophages with different plaque sizes and comparison of lysis kinetics after simultaneous and sequential phage addition. PHAGE 1, 149–157.
Artawinata, P.C., Lorraine, S., Waturangi, D.E., 2023. Isolation and characterization of bacteriophages from soil against food spoilage and foodborne pathogenic bacteria. Sci. Rep. 13, 9282.
Baker-Austin, C., Oliver, J.D., Alam, M., Ali, A., Waldor, M.K., Qadri, F., Martinez-Urtaza, J., 2018. *Vibrio* spp. infections. Nat. Rev. Dis. Prim. 4, 8.
Bankevich, A., Nurk, S., Antipov, D., Gurevich, A.A., Dvorkin, M., Kulikov, A.S., Lesin, V. M., Nikolenko, S.I., Pham, S., Prjibelski, A.D., Pyshkin, A.V., Sirotkin, A.V., Vyahhi, N., Tesler, G., Alekseyev, M.A., Pevzner, P.A., 2012. SPAdes: a new genome assembly algorithm and its applications to single-cell sequencing. J. Comput. Biol. 19, 455–477.
Bolger, A.M., Lohse, M., Usadel, B., 2014. Trimmomatic: a flexible trimmer for Illumina sequence data. Bioinformatics 30, 2114–2120.
Bonnin-Jusserand, M., Copin, S., Le Bris, C., Brauge, T., Gay, M., Brisabois, A., Grard, T., Midelet-Bourdin, G., 2019. *Vibrio* species involved in seafood-borne outbreaks (*Vibrio cholerae*, *V. parahaemolyticus* and *V. vulnificus*): review of microbiological versus recent molecular detection methods in seafood products. Crit. Rev. Food Sci. Nutr. 59, 597–610.
Bouras, G., Nepal, R., Houtak, G., Psaltis, A.J., Wormald, P.J., Vreugde, S., 2023. Pharokka: a fast scalable bacteriophage annotation tool. Bioinformatics 39, 1–4.
Bryner, J.H., Ritchie, A.E., Foley, J.W., Berman, D.T., 1970. Isolation and characterization of a bacteriophage for *Vibrio fetus*. J. Virol. 6, 94–99.
Bull, J.J., Vegge, C.S., Schmerer, M., Chaudhry, W.N., Levin, B.R., 2014. Phenotypic resistance and the dynamics of bacterial escape from phage control. PLoS One 9, e94690.
Bushnell, B., Rood, J., Singer, E., 2017. BBMerge – accurate paired shotgun read merging via overlap. PLoS One 12, 1–15.
Butt, A.A., Aldridge, K.E., Sanders, C.V., 2004. Infections related to the ingestion of seafood part I: viral and bacterial infections. Lancet Infect. Dis. 4, 201–212.
Cai, R., Wang, G., Le, S., Wu, M., Cheng, M., Guo, Z., Ji, Y., Xi, H., Zhao, C., Wang, X., Xue, Y., Wang, Z., Zhang, H., Fu, Y., Sun, C., Feng, X., Lei, L., Yang, Y., ur Rahman, S., Liu, X., Han, W., Gu, J., 2019. Three capsular polysaccharide synthesis-related glucosyltransferases, GT-1, GT-2 and WcaJ, are associated with virulence and phage sensitivity of *Klebsiella pneumoniae*. Front. Microbiol. 10.
Chaudhary, V., Kajla, P., Lather, D., Chaudhary, N., Dangi, P., Singh, P., Pandiselvam, R., 2024. Bacteriophages: a potential game changer in food processing industry. Crit. Rev. Biotechnol. 44, 1325–1349.
Chen, Y., Liu, X.-M., Yan, J.-W., Li, X.-G., Mei, L.-L., Ma, Q.-F., Ma, Y., 2010. Foodborne pathogens in retail oysters in south China. Biomed. Environ. Sci. 23, 32–36.
Chhibber, S., Kaur, S., Kumari, S., 2008. Therapeutic potential of bacteriophage in treating *Klebsiella pneumoniae* B5055-mediated lobar pneumonia in mice. J. Med. Microbiol. 57, 1508–1513.
Cornelissen, A., Ceyssens, P.-J., T'Syen, J., Van Praet, H., Noben, J.-P., Shaburova, O.V., Krylov, V.N., Volckaert, G., Lavigne, R., 2011. The T7-related *Pseudomonas putida* phage φ15 displays virion-associated biofilm degradation properties. PLoS One 6, e18597.
Costa, P., Pereira, C., Gomes, A.T.P.C., Almeida, A., 2019. Efficiency of single phage suspensions and phage cocktail in the inactivation of *Escherichia coli* and *Salmonella* Typhimurium: an *in vitro* preliminary study. Microorganisms 7, 94.
Costa, P., Gomes, A.T.P.C., Braz, M., Pereira, C., Almeida, A., 2021. Application of the resazurin cell viability assay to monitor *Escherichia coli* and *Salmonella typhimurium* inactivation mediated by phages. Antibiotics 10.
Costa, P., Pereira, C., Romalde, J.L., Almeida, A., 2024. A game of resistance: war between bacteria and phages and how phage cocktails can be the solution. Virology 599, 110209.
Dallal, M.M.S., Nikkhahi, F., Alimohammadi, M., Douraghi, M., Rajabi, Z., Foroushani, A. R., Azimi, A., Fardsanei, F., 2019. Phage therapy as an approach to control *Salmonella enterica* serotype Enteritidis infection in mice. Rev. Soc. Bras. Med. Trop. 52.
De Melo Silva, A.C.M., Do Nascimento, D.L., Machado, R.Z., Costa, F.N., 2014. Caracterização de *Aeromonas* spp. isoladas de amostras de ostras e água por método microbiológico e molecular. Cienc. Anim. Bras. 15, 362–368.
De Silva, B.C.J., Hossain, S., Dahanayake, P.S., Lee, D.-W., Wickramanayake, M.V.K.S., Heo, G.-J., 2020. Multi-drug resistant mesophilic aeromonads isolated from marketed scallops (*Patinopecten yessoensis*) harboring resistance genes. Fish. Aquat. Life 28, 1–10.
Denes, T., Wiedmann, M., 2014. Environmental responses and phage susceptibility in foodborne pathogens: implications for improving applications in food safety. Curr. Opin. Biotechnol. 26, 45–49.
Dias, J.I.P., 2020. Diversity of Tetracycline-Resistant *Vibrio* spp. in an Estuarine Environment: *V. diabolicus* Genome Case Study. Universidade de Coimbra.
Dimitrov, D.S., 2004. Virus entry: molecular mechanisms and biomedical applications. Nat. Rev. Microbiol. 2, 109–122.
Drake, S.L., DePaola, A., Jaykus, L., 2007. An overview of *Vibrio vulnificus* and *Vibrio parahaemolyticus*. Compr. Rev. Food Sci. Food Saf. 6, 120–144.
Duarte, J., Pereira, C., Costa, P., Almeida, A., 2021. Bacteriophages with potential to inactivate *Aeromonas hydrophila* in cockles: *in vitro* and *in vivo* preliminary studies. Antibiotics 10, 710.
Dziewit, L., Radlinska, M., 2016. Two novel temperate bacteriophages co-existing in *Aeromonas* sp. ARM81 – characterization of their genomes, proteomes and DNA methyltransferases. J. Gen. Virol. 97, 2008–2022.
EFSA, E.F.S.A., ECDC, E.C. for D.P. and C, 2023. The European Union One Health 2022 Zoonoses Report. EFSA J. 21.
Endersen, L., O'Mahony, J., Hill, C., Ross, R.P., McAuliffe, O., Coffey, A., 2014. Phage therapy in the food industry. Annu. Rev. Food Sci. Technol. 5, 327–349.
European Commission, 2004a. EC Commission Regulation (EC) No 853/2004 of the European Parliament and of the Council of 29 April 2004 Laying Down Specific Hygiene Rules for on the Hygiene of Foodstuffs. European Parliament.
European Commission, 2004b. Regulation (EC) No 852/2004 of the European Parliament and of the Council of 29 April 2004 on the Hygiene of Foodstuffs. European Parliament.
European Commission, 2005. Commission Regulation (EC) No 2073/2005 of 15 November 2005 on Microbiological Criteria for Foodstuffs. European Parliament.
European Commission, 2015. Commission Regulation (EU) 2015/2285 of 8 December 2015 Amending Annex II to Regulation (EC) No 854/2004 of the European Parliament and of the Council Laying Down Specific Rules for the Organisation of Official Controls on Products of Animal Origin Intended for Human Consumption as Regards Certain Requirements for Live Bivalve Molluscs, Echinoderms, Tunicates and Marine Gastropods and Annex I to Regulation (EC) No 2073/2005 on microbiological criteria for foodstuff. European Parliament.
European Commission, 2017. Regulation (EU) 2017/625 of the European Parliament and of the Council of 15 March 2017. European Parliament.
FAO, 2024. The State of World Fisheries and Aquaculture 2024, FAO Fisheriestechnical Paper. FAO, Rome.
Finstad, S., O'Bryan, C.A., Marcy, J.A., Crandall, P.G., Ricke, S.C., 2012. *Salmonella* and broiler processing in the United States: relationship to foodborne salmonellosis. Food Res. Int. 45, 789–794.
Fogg, P.C.M., Rigden, D.J., Saunders, J.R., McCarthy, A.J., Allison, H.E., 2011. Characterization of the relationship between integrase, excisionase and antirepressor activities associated with a superinfecting Shiga toxin encoding bacteriophage. Nucleic Acids Res. 39, 2116–2129.
Gallet, R., Kannoly, S., Wang, I.-N., 2011. Effects of bacteriophage traits on plaque formation. BMC Microbiol. 11, 181.
Ge, H., Hu, M., Zhao, G., Du, Y., Xu, N., Chen, X., Jiao, X., 2020. The "fighting wisdom and bravery" of tailed phage and host in the process of adsorption. Microbiol. Res. 230, 126344.
Grim, C.J., Kozlova, E.V., Ponnusamy, D., Fitts, E.C., Sha, J., Kirtley, M.L., van Lier, C.J., Tiner, B.L., Erova, T.E., Joseph, S.J., Read, T.D., Shak, J.R., Joseph, S.W., Singletary, E., Felland, T., Baze, W.B., Horneman, A.J., Chopra, A.K., 2014. Functional genomic characterization of virulence factors from necrotizing fasciitis-causing strains of *Aeromonas hydrophila*. Appl. Environ. Microbiol. 80, 4162–4183.
Guzel, M., Yucefaydali, A., Yetiskin, S., Deniz, A., Yaşar Tel, O., Akçelik, M., Soyer, Y., 2024. Genomic analysis of *Salmonella* bacteriophages revealed multiple endolysin ORFs and importance of ligand-binding site of receptor-binding protein. FEMS Microbiol. Ecol. 100.
Hanlon, G.W., 2007. Bacteriophages: an appraisal of their role in the treatment of bacterial infections. Int. J. Antimicrob. Agents 30, 118–128.
Harrison, E., Brockhurst, M.A., 2017. Ecological and evolutionary benefits of temperate phage: what does or doesn't kill you makes you stronger. BioEssays 39.
Hawkins, C., Harper, D., Burch, D., Ånggård, E., Soothill, J., 2010. Topical treatment of *Pseudomonas aeruginosa* otitis of dogs with a bacteriophage mixture: a before/after clinical trial. Vet. Microbiol. 146, 309–313.
Hurley, A., Maurer, J.J., Lee, M.D., 2008. Using bacteriophages to modulate *Salmonella* colonization of the chicken's gastrointestinal tract: lessons learned from *in silico* and *in vivo* modeling. Avian Dis. 52, 599–607.
Hyman, P., Abedon, S.T., 2009. Practical methods for determining phage growth parameters. In: Methods in Molecular Biology, pp. 175–202.
Igler, C., 2022. Phenotypic flux: the role of physiology in explaining the conundrum of bacterial persistence amid phage attack. Virus Evol. 8, veac086.
Iwamoto, M., Ayers, T., Mahon, B.E., Swerdlow, D.L., 2010. Epidemiology of seafood-associated infections in the United States. Clin. Microbiol. Rev. 23, 399–411.
Jakočiūnė, D., Moodley, A., 2018. A rapid bacteriophage DNA extraction method. Methods Protoc. 1, 27.

Jun, J.W., Shin, T.H., Kim, J.H., Shin, S.P., Han, J.E., Heo, G.J., De Zoysa, M., Shin, G.W., Chai, J.Y., Park, S.C., 2014. Bacteriophage therapy of a *Vibrio parahaemolyticus* infection caused by a multiple-antibiotic–resistant O3:K6 pandemic clinical strain. J. Infect. Dis. 210, 72–78.
Kanayama, A., Yahata, Y., Arima, Y., Takahashi, T., Saitoh, T., Kanou, K., Kawabata, K., Sunagawa, T., Matsui, T., Oishi, K., 2015. Enterohemorrhagic *Escherichia coli* outbreaks related to childcare facilities in Japan, 2010–2013. BMC Infect. Dis. 15, 539.
Knecht, L.E., Veljkovic, M., Fieseler, L., 2020. Diversity and function of phage encoded depolymerases. Front. Microbiol. 10.
Kutter, E., 2009. Phage host range and efficiency of plating. In: Clokie, M.R., K.A.M. (Eds.), Bacteriophage: Methods and Protocols. Humana Press, pp. 141–149.
Lamont, I., Richardson, H., Carter, D.R., Egan, J.B., 1993. Genes for the establishment and maintenance of lysogeny by the temperate coliphage 186. J. Bacteriol. 175, 5286–5288.
Langmead, B., Salzberg, S.L., 2012. Fast gapped-read alignment with Bowtie 2. Nat. Methods 9, 357–359.
Lee, R., Lovatelli, A., Ababouch, L., 2008. Bivalve depuration: fundamental and practical aspects. In: FAO Fisheries Technical Paper, Rome.
Li, K., Barksdale, L., Garmise, L., 1961. Phenotypic alterations associated with the bacteriophage carrier state of *Shigella dysenteriae*. J. Gen. Microbiol. 24, 355–367.
Li, P., Zhang, X., Xie, X., Tu, Z., Gu, J., Zhang, A., 2020. Characterization and whole-genome sequencing of broad-host-range *Salmonella*-specific bacteriophages for bio-control. Microb. Pathog. 143, 104119.
Litt, P.K., Saha, J., Jaroni, D., 2018. Characterization of bacteriophages targeting non-O157 Shiga toxigenic *Escherichia coli*. J. Food Prot. 81, 785–794.
Łobocka, M., Dąbrowska, K., Górski, A., 2021. Engineered bacteriophage therapeutics: rationale, challenges and future. BioDrugs 35, 255–280.
Louvado, A., Santos, A.L., Coelho, F., Sousa, S., Moreira, A., Gomes, F., Almeida, A., Gomes, N.C.M., Cunha, Â., 2010. Isolation of surfactant-resistant bacteria from the surface microlayer. Interdiscip. Stud. Environ. Chem. — Biol. Responses Contam. 22, 89–95.
Martínez, O., Rodríguez-Calleja, J.M., Santos, J.A., Otero, A., García-López, M.L., 2009. Foodborne and indicator bacteria in farmed molluscan shellfish before and after depuration. J. Food Prot. 72, 1443–1449.
Mateus, L., Costa, L., Silva, Y.J., Pereira, C., Cunha, A., Almeida, A., 2014. Efficiency of phage cocktails in the inactivation of *Vibrio* in aquaculture. Aquaculture 424–425, 167–173.
Mirzaei, M.K., Nilsson, A.S., 2015. Isolation of phages for phage therapy: a comparison of spot tests and efficiency of plating analyses for determination of host range and efficacy. PLoS One 10, e0118557.
Monteiro, R., Pires, D.P., Costa, A.R., Azeredo, J., 2019. Phage therapy: going temperate? Trends Microbiol. 27, 368–378.
Moreno Roldán, E., Rodríguez, E.E., Vicente, C.N., Navajas, M.F., Abril, O.M., 2011. Microbial contamination of bivalve mollusks used for human consumption. J. Food Saf. 31, 257–261.
Nakai, T., 2010. Application of bacteriophages for control of infectious diseases in aquaculture. In: Sabour, P., Griffiths, M. (Eds.), Bacteriophages in the Control of Food and Waterborne Pathogens. ASM Press, Washington, DC, USA, USA, pp. 257–272.
Nayfach, S., Camargo, A.P., Schulz, F., Eloe-Fadrosh, E., Roux, S., Kyrpides, N.C., 2021. CheckV assesses the quality and completeness of metagenome-assembled viral genomes. Nat. Biotechnol. 39, 578–585.
Neufing, P.J., Shearwin, K.E., Egan, J.B., 2001. Establishing lysogenic transcription in the temperate coliphage 186. J. Bacteriol. 183, 2376–2379.
Oliveira, H., Sillankorva, S., Merabishvili, M., Kluskens, L.D., Azeredo, J., 2015. Unexploited opportunities for phage therapy. Front. Pharmacol. 6, 1–4.
Oliveira, A., Sousa, J.C., Silva, A.C., Melo, L.D.R., Sillankorva, S., 2018. Chestnut honey and bacteriophage application to control *Pseudomonas aeruginosa* and *Escherichia coli* biofilms: evaluation in an *ex vivo* wound model. Front. Microbiol. 9.
Payne, R.J.H., Jansen, V.A.A., 2003. Pharmacokinetic principles of bacteriophage therapy. Clin. Pharmacokinet. 42, 315–325.
Pereira, C., Silva, Y., Santos, A.L., Cunha, Â., Gomes, N.C.M., Almeida, A., 2011. Bacteriophages with potential for inactivation of fish pathogenic bacteria: survival, host specificity and effect on bacterial community structure. Mar. Drugs 9, 2236–2255.
Pereira, C., Moreirinha, C., Lewicka, M., Almeida, P., Clemente, C., Cunha, Â., Delgadillo, I., Romalde, J.L., Nunes, M.L., Almeida, A., 2016a. Bacteriophages with potential to inactivate *Salmonella* Typhimurium: use of single phage suspensions and phage cocktails. Virus Res. 220, 179–192.
Pereira, S., Pereira, C., Santos, L., Klumpp, J., Almeida, A., 2016b. Potential of phage cocktails in the inactivation of *Enterobacter cloacae* — an *in vitro* study in a buffer solution and in urine samples. Virus Res. 211, 199–208.
Pereira, C., Moreirinha, C., Lewicka, M., Almeida, P., Clemente, C., Romalde, J.L., Nunes, M.L., Almeida, A., 2017a. Characterization and *in vitro* evaluation of new bacteriophages for the biocontrol of *Escherichia coli*. Virus Res. 227, 171–182.
Pereira, C., Moreirinha, C., Teles, L., Rocha, R.J.M.M., Calado, R., Romalde, J.L., Nunes, M.L., Almeida, A., 2017b. Application of phage therapy during bivalve depuration improves *Escherichia coli* decontamination. Food Microbiol. 61, 102–112.
Pereira, C., Costa, P., Duarte, J., Balcão, V.M., Almeida, A., 2021. Phage therapy as a potential approach in the biocontrol of pathogenic bacteria associated with shellfish consumption. Int. J. Food Microbiol. 338, 108995.
Potasman, I., Paz, A., Odeh, M., 2002. Infectious outbreaks associated with bivalve shellfish consumption: a worldwide perspective. Clin. Infect. Dis. 35, 921–928.
Rafiei, S., Bouzari, M., 2024. Genomic analysis of vB_PaS-HSN4 bacteriophage and its antibacterial activity (*in vivo* and *in vitro*) against *Pseudomonas aeruginosa* isolated from burn. Sci. Rep. 14, 2007.
Rai, S., Tyagi, A., Naveen Kumar, B.T., Reddy S, V.K., 2023. Isolation and characterization of *Aeromonas hydrophila* lytic phage, and evaluation of a phage cocktail against *A. hydrophila* contamination in fish fillet. Food Control 145, 109460.
Rodin, S.N., Ratner, V.A., 1983. Some theoretical aspects of protein coevolution in the ecosystem "phage-bacteria" II. The deterministic model of microevolution. J. Theor. Biol. 100, 197–210.
Rong, R., Lin, H., Wang, J., Khan, M.N., Li, M., Naseem, M., Li, M., Khan, M.N., Li, M., 2014. Reductions of *Vibrio parahaemolyticus* in oysters after bacteriophage application during depuration. Aquaculture 418–419, 171–176.
Salim, A., Madhavan, A., Subhash, S., Prasad, M., Nair, B.G., Pal, S., 2022. *Escherichia coli* ST155 as a production-host of three different polyvalent phages and their characterisation with a prospect for wastewater disinfection. Sci. Rep. 12, 19406.
Sambrook, J., Russel, D.W., 2001. Molecular Cloning: A Laboratory Manual. Cold Spring Harbor Laboratory Press, Cold Spring Harbor, NY, USA.
Shen, A., Millard, A., 2021. Phage genome annotation: where to begin and end. PHAGE Ther. Appl. Res. 2, 183–193.
Shymialevich, D., Wójcicki, M., Wardaszka, A., Świder, O., Sokołowska, B., Błażejak, S., 2022. Application of lytic bacteriophages and their enzymes to reduce saprophytic bacteria isolated from minimally processed plant-based food products—*in vitro* studies. Viruses 15, 9.
Silva, I., Tacão, M., Tavares, R.D.S., Miranda, R., Araújo, S., Manaia, C.M., Henriques, I., 2018. Fate of cefotaxime-resistant Enterobacteriaceae and ESBL-producers over a full-scale wastewater treatment process with UV disinfection. Sci. Total Environ. 639, 1028–1037.
Skehel, J.J., Wiley, D.C., 2000. Receptor binding and membrane fusion in virus entry: the influenza hemagglutinin. Annu. Rev. Biochem. 69, 531–569.
Sobhy, H., Soliman, E.A., Abd El-Tawab, A.A., Elhofy, F.I., Askora, A., El-Nahas, E.M., Wareth, G., Ahmed, W., 2021. Isolation, characterization, and efficacy of three lytic phages infecting multidrug-resistant *Salmonella* serovars from poultry farms in Egypt. Arch. Razi Inst. 76, 507–519.
Sobrinho, P.D.S.C., Destro, M.T., Franco, B.D.G.M., Landgraf, M., 2010. Correlation between environmental factors and prevalence of *Vibrio parahaemolyticus* in oysters harvested in the southern coastal area of São Paulo State, Brazil. Appl. Environ. Microbiol. 76, 1290–1293.
Ssekatawa, K., Byarugaba, D.K., Kato, C.D., Wampande, E.M., Ejobi, F., Tweyongyere, R., Nakavuma, J.L., 2021. A review of phage mediated antibacterial applications. Alexandria J. Med. 57, 1–20.
Storms, Z.J., Sauvageau, D., 2015. Modeling tailed bacteriophage adsorption: insight into mechanisms. Virology 485, 355–362.
Storms, Z.J., Smith, L., Sauvageau, D., Cooper, D.G., 2012. Modeling bacteriophage attachment using adsorption efficiency. Biochem. Eng. J. 64, 22–29.
Stuer-Lauridsen, B., Janzen, T., Schnabl, J., Johansen, E., 2003. Identification of the host determinant of two prolate-headed phages infecting *Lactococcus lactis*. Virology 309, 10–17.
Sun, Z., Mandlaa, Wen, H., Ma, L., Chen, Z., 2022. Isolation, characterization and application of bacteriophage PSDA-2 against *Salmonella* Typhimurium in chilled mutton. PLoS One 17, e0262946.
Tacão, M., Correia, A., Henriques, I.S., 2015. Low prevalence of carbapenem-resistant bacteria in river water: resistance is mostly related to intrinsic mechanisms. Microb. Drug Resist. 21, 497–506.
Tan, C.W., Rukayadi, Y., Hasan, H., Abdul-Mutalib, N.-A., Jambari, N.N., Hara, H., Thung, T.Y., Lee, E., Radu, S., 2021. Isolation and characterization of six *Vibrio parahaemolyticus* lytic bacteriophages from seafood samples. Front. Microbiol. 12.
Terzian, P., Ndela, E.O., Galiez, C., Lossouarn, J., Bucio, R.E.P., Mom, R., Toussaint, A., Petit, M.-A., Enault, F., 2021. PHROG: families of prokaryotic virus proteins clustered using remote homology. NAR Genom. Bioinform. 3, lqab067.
Vincent, A.T., Paquet, V.E., Bernatchez, A., Tremblay, D.M., Moineau, S., Charette, S.J., 2017. Characterization and diversity of phages infecting *Aeromonas salmonicida* subsp. *salmonicida*. Sci. Rep. 7, 7054.
Walker, B.J., Abeel, T., Shea, T., Priest, M., Abouelliel, A., Sakthikumar, S., Cuomo, C.A., Zeng, Q., Wortman, J., Young, S.K., Earl, A.M., 2014. Pilon: an integrated tool for comprehensive microbial variant detection and genome assembly improvement. PLoS One 9.
Wick, R.R., Schultz, M.B., Zobel, J., Holt, K.E., 2015. Bandage: interactive visualization of de novo genome assemblies. Bioinformatics 31, 3350–3352.
Wick, R.R., Judd, L.M., Gorrie, C.L., Holt, K.E., 2017. Unicycler: resolving bacterial genome assemblies from short and long sequencing reads. PLoS Comput. Biol. 13, e1005595.
Wong, C.L., Sieo, C.C., Tan, W.S., Abdullah, N., Hair-Bejo, M., Abu, J., Ho, Y.W., 2014. Evaluation of a lytic bacteriophage, Φ st1, for biocontrol of *Salmonella enterica* serovar Typhimurium in chickens. Int. J. Food Microbiol. 172, 92–101.
Xu, Y., Sun, J., Hu, J., Bao, Z., Wang, M., 2023. Characterization and preliminary application of a novel lytic *Vibrio parahaemolyticus* bacteriophage vB_VpaP_SJSY21. Int. J. Mol. Sci. 24, 17529.
Ye, Y., Chen, H., Huang, Q., Huang, S., He, J., Zhang, J., Wu, Q., Li, X., Hu, W., Yang, M., 2022. Characterization and genomic analysis of novel *Vibrio parahaemolyticus* phage vB_VpaP_DE10. Viruses 14, 1609.
Zannella, C., Mosca, F., Mariani, F., Franci, G., Folliero, V., Galdiero, Marilena, Tiscar, P. G., Galdiero, Massimiliano, 2017. Microbial diseases of bivalve mollusks: infections, immunology and antimicrobial defense. Mar. Drugs 15, 182.
Zhang, Y., Chu, M., Liao, Y.-T., Salvador, A., Wu, V.C.H., 2024a. Characterization of two novel *Salmonella* phages having biocontrol potential against *Salmonella* spp. in gastrointestinal conditions. Sci. Rep. 14, 12294.

Zhang, C., Li, X., Li, S., Yin, H., Zhao, Z., 2024b. Characterization and genomic analysis of a broad-spectrum lytic phage PG288: a potential natural therapy candidate for *Vibrio* infections. Virus Res. 341, 199320.
Zhou, Y., Wan, Q., Bao, H., Guo, Y., Zhu, S., Zhang, H., Pang, M., Wang, R., 2022. Application of a novel lytic phage vB_EcoM_SQ17 for the biocontrol of Enterohemorrhagic *Escherichia coli* O157:H7 and Enterotoxigenic *E. coli* in food matrices. Front. Microbiol. 13.
Zhou, S., Liu, Z., Song, J., Chen, Y., 2023. Disarm the bacteria: what temperate phages can do. Curr. Issues Mol. Biol. 45, 1149–1167.